Renewable and Sustainable Energy Reviews 16 (2012) 3383–3390

Contents lists available at SciVerse ScienceDirect

Renewable and Sustainable Energy Reviews

journal homepage: www.elsevier.com/locate/rser

Solar chimney power plant performance in Iran

A. Asnaghi*, S.M. Ladjevardi

Renewable Energy Department, Energy and Environment Research Center, Niroo Research Institute, Ministry of Energy, P.O. Box 14665, 517 Tehran, Iran

ARTICLE INFO

Article history:
Received 28 January 2012
Accepted 5 February 2012
Available online 28 March 2012

Keywords:
Solar chimney
Solar tower
Thermal power plant
Solar energy
Electricity production

ABSTRACT

A solar chimney power plant (SCPP) is proposed to be built as the first national SCPP in central regions of Iran. Studies of DLR MED-CSP project show that Iran can be a part of the Mediterranean solar power generation chain in 2050 to provide electrical power demand of Europe. High direct solar radiation and available desert lands in Iran are factors to encourage the full development of solar power plants like solar chimney power plants for the thermal and electrical productions of energy for various uses. The interested region is the central region of Iran where solar radiation and global insolation are much better than other areas. However, to evaluate SCPP performance and power generation throughout Iran, 12 different areas across the country are considered. The obtained results clear that solar chimney power plants can produce from 10 to 28 MWh/month of electrical power. This power production is sufficient for the needs of the isolated areas and can even used to feed the grid.

Contents

1. Introduction

Increase in world population and living standards, growing world electricity consumption, the limited amount of existing fossil fuel, and the contamination of the environment let us know the necessity of using efficient electricity generation systems. By releasing greenhouse gases, utilization of fossil fuels has induced considerable climate change such as warming the atmosphere. Increase in greenhouse gases may cause several negative impacts including receding of glaciers, loss of biodiversity, extinction of animals, and loss of productive forests, acidification of oceans, killing of heat waves, and retreat of butterflies up mountainsides worldwide. Renewable energy sources can play a great role in solving the above problems in the future. Solar chimney power plant which absorbs direct and diffused solar radiation and converts parts of solar energy into electric power offers interesting opportunities to use pollution free resources of energy [1].

Solar chimney power plant can make significant contributions to the energy supplies of those countries where solar radiation is

* Corresponding author. Tel.: +98 21 88361601.
E-mail addresses: Asnaghi_a@yahoo.com, aasnaghi@nri.ac.ir (A. Asnaghi).

1364-0321/$ – see front matter © 2012 Elsevier Ltd. All rights reserved.
doi:10.1016/j.rser.2012.02.017

Nomenclature

u	velocity in radial direction
v	velocity in tangential direction
V	wind velocity
t	time
r	radial direction
y	tangential direction
P	pressure
T	temperature
Ra	Rayleigh number
Pr	Prandtl number
g	gravity
a	thermal diffusivity
q	irradiation
h	convection heat transfer coefficient
ρ	density
ρ_0	reference density
μ	viscosity
β	thermal expansion coefficient
τ	transmission coefficient
η	efficiency
$\forall$	air volume flow rate
δ	difference
ε	emissivity

Subscript

cr	collector roof
amb	ambient
s	surface
t	turbine

highly available and there is plenty of desert land, which is not being utilized.

Currently, solar energy is still underutilized and unfortunately occupies a smaller portion of the total energy demand. Due to the ever decreasing amount of available conventional (fossil) fuels, renewable solar energy has become exceedingly important and more commercially affordable. This change has resulted in a strategic European decision to utilize clean technologies, which was confirmed by the signing of the Kyoto Protocol. In the near future, Europe plans to significantly reduce its usage of fossil fuels, but it does not plan to abandon fossil fuel technologies. Currently, the EU plans to provide 20% of electric energy and 30% of thermal energy from renewable energy sources by the year 2020 [2]. Moreover, to satisfy future electrical energy demand, EU plans to develop solar power plants in other countries like Mediterranean, and Middle East countries. In DLR MED-CSP project, different countries, e.g. Iran, was analyzed to estimate potential of electrical power generation from renewable energies [2]. Studies of this project and other national performed projects show that there are suitable regions in Iran which have high potential for electricity generation from solar energy.

In the central regions of Iran, solar radiation is highly available throughout the year, as well as extensive desert areas. These conditions are favorable for development of a solar chimney power plant. In addition to power generation, SCPP can be applied for agricultural purposes in these less developed regions. However, to evaluate the available potential throughout country, 12 different regions across Iran have been selected. The dimension of SCPP which is used to compare potential of different locations is the same as Mansanares prototype [3,4].

Numerical simulation is used to investigate SCPP performance in 12 selected regions. Power generation of each region is

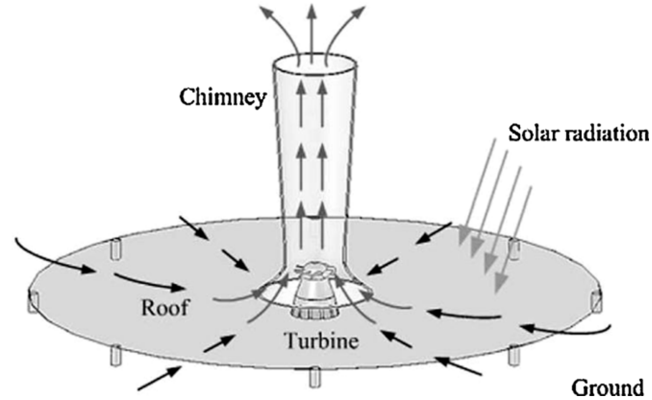


Fig. 1. Solar chimney power plant schematic layout [6].

compared with other regions and the power potential of SCPP in Iran is evaluated in this paper.

2. Solar chimney power plant (SCPP)

A solar chimney power plant consists of three major parts, the collector, the chimney and the power conversion unit (PCU) which includes one or several turbine generators. Using the energy storage layer, secondary roof, and solar pond are proposed to adjust the power production uniformity of the SCPP during the day and the night [1,5].

SCPP works like a natural power generator that uses solar radiation energy to increase the internal energy of the flowing air. In this system, the solar radiation heats the air below the transparent collector roof, creating a gradient of temperature. Because the density of air is proportional to its temperature, the temperature gradient will create the density gradient. The collector slopes from its inlet to its center, so buoyancy effects will force air to flow from inlet of the collector to entry of chimney where the flowing air will rotate a turbine to produce power as it is shown in Fig. 1.

Basic study on the solar chimney concept was first performed by Haaf et al. [3,4]. They began the construction of a pilot solar chimney power plant in Mansanares, Spain. The chimney had a height of 200 m and a diameter of 10 m. The collector area radius was 122 m. The maximum power output was measured up to 50 kW [5].

After building the Spanish solar chimney prototype, the device was considered as the fundamental and experimental basis for more studies. Considerable efforts were made in analyzing the performance of the chimney power plant in order to prove the feasibility as well as the profitability of this kind of power plant comparing with the traditional ones. As it is expected, these studies showed that the effectiveness of the solar chimney is strongly influenced by received solar energy. Pasumarthi and Sherif [7,8] have shown that solar chimney technology can be a viable alternative technology adapted to hot climate areas such as of Florida. They also developed a mathematical model to estimate the temperature and power generation of solar chimney power plants.

It has been shown that the most important physical elements in a solar chimney are the tower dimensions as they cause the most significant influence on the flow patterns. Another important factor is the collector roof shape. Researches show that greater power production is feasible by optimizing the collector roof shape and height.

The characteristics of the SCPP are listed below [9].

- Efficient solar radiation absorption: The hot air collector used in the system, can absorb both direct and diffused radiation. Thus the solar chimney can operate on both clear and overcast days.

- Free dual functions, natural energy storage and greenhouse effect: The collector provides storage for natural energy, as the ground under the transparent cover can absorb some of the radiated energy during the day and releases it into the collector at night. Thus solar chimneys also produce a significant amount of electricity at night. The collector itself can also be used as a greenhouse, which will benefit agriculture production accordingly.
- SCPP can operate with low operational cost: Unlike some conventional power plants, and also other solar–thermal type power stations, SCPP do not require any cooling water. This is a key advantage in desert lands where there have already been problems with potable water.
- Construction of a SCPP costs low: The building materials, mainly concrete and transparent materials, needed for solar chimneys are available everywhere in almost sufficient capacities. The most important part is that no investment in a high-tech manufacturing plant is needed, as both wind turbine technology and solar collectors manufacturing are well-developed.

3. SCPP in Iran

Evaluation of SCPP performances in some regions of Iran has been studied previously [10]. In the previous work, due to the lack of precise environmental information, the considered values for affective parameters such as solar radiation, temperature and wind speed have been calculated approximately. Besides, considered regions usually selected without considering geographical conditions, grid, free lands' availability, and economy conditions of the regions. In the current study, it is aimed to move forward previous research. NRI solar field software which is derived from several years environmental average values is used to derive and calculate monthly average solar radiation, wind speed, duration of sunshine hours, and other geographical data [11]. In the following sections, more details about this atlas have been provided.

In the current investigation, 12 regions have been selected for feasibility study of constructing a SCPP. Information of these regions is presented in Table 1. Annual solar radiation of the major of the selected regions is more than 6500 MJ/m^2, and sunshine duration lies between 2400 h and 3400 h per year. Iranshahr, Jahrom, Bam, Zabol, and Dashtestan have higher annual solar radiation comparing to the other selected regions. Zabol has higher average annual wind speed which may lead to increase heat loss from the roof of the collector. Ardabil presents poorest conditions with the lowest annual solar radiation and annual sunshine duration. The selected regions are presented in Fig. 2 which is derived from Google Map. As it can be observed, selected regions have been chosen from different locations of country.



Fig. 2. Locations of 12 selected regions for SCPP performance evaluation in Iran.

4. Mathematical model and boundary conditions

Finite volume method is employed to discretize the governing equations. Due to the low variations in the air density, the flow is considered incompressible while the compressibility effects are modeled by Boussinesq model. The soil is considered as energy storage layer. It is assumed that soil will attract all passed solar energy from the transparent roof and then will transfer it to the air inside the collector.

4.1. Geometry and boundary conditions

To verify the simulation assumptions and procedure, the Spanish SCPP has been considered as the test case. The experimental data of temperature increase in the collector and average velocity in the base of the chimney are available to compare with numerical results. Dimensions of the test case are as follows: height of chimney, 200 m; diameter of chimney, 10 m; radius of collector, 122 m; height from the inlet to its center, 2–6 m; thickness of the energy storage layer, 5 m. In Fig. 3, the dimensions and geometry of the solar chimney power plant are presented schematically.

Table 1
Annual global solar radiation and atmospheric conditions of 12 selected regions in Iran.

Region	Province	Longitude	Latitude	Average annual temperature (K)	Average annual wind speed (m/s)	Annual sunshine duration (h)	Annual solar radiation (MJ/m^2)
Bam	KERMAN	58°21′	29°6′	23.08	2.92	3381.6	7307.91
Tabas	YAZD	56°55′	33°35′	22.42	1.51	3322.3	6843.142
Jahrom	FARS	53°33′	28°30′	25.04	2.07	3398.4	7404.197
Zabol	SISTAN-VA BALUCHESTAN	61°29′	31°1′	22.73	5.23	3180.8	7218.597
Dashtestan	BUSHEHR	51°12′	29°16′	24.67	2.78	3172.3	7155.944
Ardabil	ARDABIL	48°18′	38°15′	9.87	3.22	2400.9	4650.103
Divandare	KORDESTAN	47°1′	35°54′	11.06	2.58	2940.7	6274.696
Iranshahr	SISTAN-VA BALUCHESTAN	60°41′	27°12′	27.52	2.05	3279.2	7481.012
KhorramAbad	LORESTAN	48°21′	33°29′	16.98	2.00	3044	6651.087
Sabzevar	KHORASAN-E-RAZAVI	57°40′	36°12′	17.18	2.86	3026.1	6295.426
Varamin	TEHRAN	51°39′	35°19′	16.76	1.57	3038.9	6431.607
Yazd	YAZD	54°22′	31°53′	19.58	2.68	3252.7	6890.823

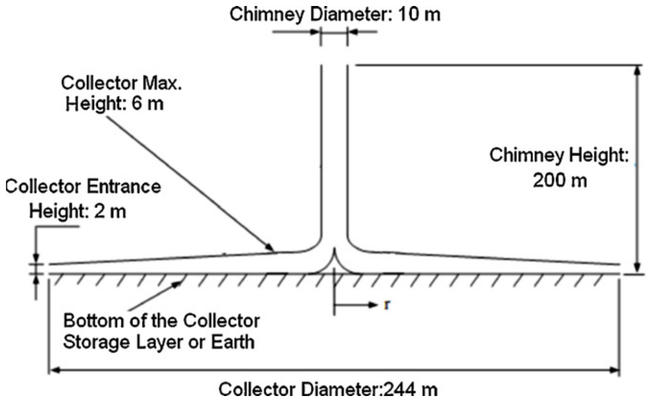


Fig. 3. Dimensions and geometry of the solar chimney power plant.

A solar chimney plant with the similar fundamental dimensions like the Spanish solar chimney plant will be built in Iran. The analyses of overall performance considering the radiation variations through the year in the selected regions have been provided in this paper. Ambient temperature, wind velocity, and other environmental data have been used as the monthly average data.

In the project proposal of Iranian SCPP, it is considered that the soil will be used as the energy storage layer. Moreover, the collector will be used as a green house for agricultural uses. To reduce the energy loss caused by resistance, the collector and the chimney are smoothly connected. Besides, shrink flow passage is considered at the bottom of chimney. The roof material is transparent glass having the transition coefficient equal to 0.85.

Boundary conditions are set as follows: the outer surface of collector roof has free convection heat transfer with the ambient air. The coefficient of convection is calculated based on the air velocity which will be described in the heat transfer mechanism section. The real measured ambient temperature, and wind velocity values are provided to increase accuracy of simulations. The pressure-inlet boundary is considered for both the collector inlet and the chimney outlet. The pressure and temperature values at the inlet and the outlet boundaries are set as equal to the ambient pressure and temperature. The chimney wall can be set as an adiabatic boundary [12]. Solar radiation which passes through the transparent roof can be considered as a heat source for the ground thin layer [13]. The employed mesh is presented in Fig. 4.

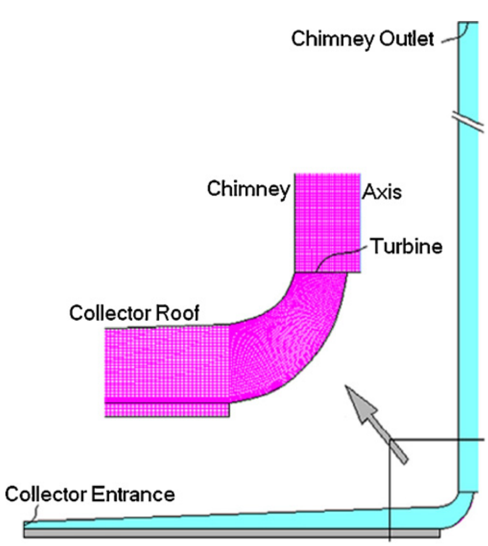


Fig. 4. Employed mesh for simulation of Solar chimney power plant.

4.2. Governing equations

Due to the flow pattern inside the solar chimney, the geometry can be considered as a 2-d axisymmetry flow. The governing equations concerning flow inside the solar chimney in the cylindrical coordinate are as follow:

$$\frac{\partial(\rho)}{\partial t} + \frac{1}{r}\frac{\partial}{\partial r}(\rho r u) + \frac{\partial(\rho v)}{\partial y} = 0 \quad (1)$$

$$\frac{\partial(\rho u)}{\partial t} + \frac{1}{r}\frac{\partial}{\partial r}(\rho r u u) + \frac{\partial(\rho u v)}{\partial y} = -\frac{\partial P}{\partial r} + \frac{1}{r}\frac{\partial}{\partial r}\left(\mu r \frac{\partial u}{\partial r}\right) + \frac{\partial}{\partial y}\left(\mu \frac{\partial u}{\partial y}\right) - 2\mu \frac{u}{r^2} \quad (2)$$

$$\frac{\partial(\rho v)}{\partial t} + \frac{1}{r}\frac{\partial}{\partial r}(\rho r u v) + \frac{\partial(\rho v v)}{\partial y} = -\frac{\partial P}{\partial y} + \frac{1}{r}\frac{\partial}{\partial r}\left(\mu r \frac{\partial v}{\partial r}\right) + \frac{\partial}{\partial y}\left(\mu \frac{\partial v}{\partial y}\right) + (\rho_0 - \rho)g \quad (3)$$

$$\frac{\partial(\rho T)}{\partial t} + \frac{1}{r}\frac{\partial}{\partial r}(\rho r u T) + \frac{\partial(\rho v T)}{\partial y} = \frac{1}{r}\frac{\partial}{\partial r}\left(r \frac{\lambda}{C_p}\frac{\partial T}{\partial r}\right) + \frac{\partial}{\partial y}\left(\frac{\lambda}{C_p}\frac{\partial T}{\partial y}\right) \quad (4)$$

In the natural convection, the strength of the buoyancy-induced flow is measured by the Rayleigh number (Ra):

$$Ra = \frac{g\beta \Delta T L^a}{a\nu} \quad (5)$$

where ΔT is the maximum temperature difference of the system. L, a and β are the mean collector height, the thermal diffusivity and the thermal expansion coefficient, respectively. In the whole, collector and chimney analysis shows that $Ra > 10^{10}$, thereby, fluid flow in the regions may be turbulent. To consider turbulence effects, standard k–ε method is utilized. By solving the two following equations, effective viscosity will be calculated based on the constant air viscosity and flow turbulent induced viscosity.

$$\frac{\partial(\rho k)}{\partial t} + \frac{1}{r}\frac{\partial}{\partial r}(\rho r k u) + \frac{\partial(\rho k v)}{\partial y} = \frac{1}{r}\frac{\partial}{\partial r}\left(r\left(\mu + \frac{\mu_t}{\sigma_k}\right)\frac{\partial k}{\partial r}\right) + \frac{\partial}{\partial y}\left(\left(\mu + \frac{\mu_t}{\sigma_k}\right)\frac{\partial k}{\partial y}\right) + G_k + \beta g \frac{\mu_t}{Pr_{kt}}\frac{\partial T}{\partial y} - \rho\varepsilon \quad (6)$$

$$\frac{\partial(\rho \varepsilon)}{\partial t} + \frac{1}{r}\frac{\partial}{\partial r}(\rho r \varepsilon u) + \frac{\partial(\rho \varepsilon v)}{\partial y} = \frac{1}{r}\frac{\partial}{\partial r}\left(r\left(\mu \frac{\mu_t}{\sigma_\varepsilon}\right)\frac{\partial \varepsilon}{\partial r}\right) + \frac{\partial}{\partial y}\left(\left(\mu + \frac{\mu_t}{\sigma_\varepsilon}\right)\frac{\partial \varepsilon}{\partial y}\right) + G_k C_{1\varepsilon}\left(\frac{\varepsilon}{k}\right) - C_{2\varepsilon}\rho\left(\frac{\varepsilon^2}{k}\right) \quad (7)$$

The constants of the above equations are considered as follows:

$$C_{1\varepsilon} = 1.44, \quad C_{2\varepsilon} = 1.92, \quad \sigma_\varepsilon = 1.3, \quad \sigma_k = 1.0, \quad (8)$$

4.3. Heat transfer mechanisms

4.3.1. Roof of collector

- Sun radiation: Although the roof of the collector is made of transparent materials, it cannot pass all the received sun radiations. Therefore, we have to consider absorption, reflection and transmission. In most literature due to small value, the reflection of the outer surface of the roof is neglected. Furthermore, the scattering effects and absorption of air inside the collector have small

effects on the total energy balance calculation. So, it is assumed that all the transmitted radiation from the roof will reach to the soil. The absorbed energy of roof due to sun radiation will be:

$$\text{Absored energy from sun radition by roof} = (1-\tau)q \quad (9)$$

where τ is the transmission coefficient of the roof materials.

- Free convection with the ambient air: Due to absorbing some parts of sun radiation, the outer surface of the roof has higher temperature than the ambient air. This condition will lead to free convection heat transfer between the outer surface of the roof and the ambient air. The heat transfer coefficient is calculated based on the ambient air velocity as follow [14]:

$$h_{cr} = 5.67 + 3.86V_{amb} \quad (10)$$

where V_w is the ambient air velocity.

- Conduction heat transfer in the roof: Because of the small thickness of the roof, the temperature difference between two sides of the roof will be negligible and therefore, the conduction heat transfer will be omitted.
- Radiation between the outer surface of the roof with the sky: The irradiative heat transfer coefficient is:

$$h_{r,g-s} = \frac{1}{2}\sigma\varepsilon_g(1-\cos\beta)(T_g + T_{sky})(T_g^2 + T_{sky}^2) \quad (11)$$

where β is the angle between the roof and the sky, T_g is the temperature of the cover, and T_{sky} is the equivalent temperature of the sky which can be defined as follow:

$$T_{sky} = 0.0552T_{amb}^{1.5} \quad (12)$$

- Radiation between the inner surface of the roof with the soil (or absorber): Due to temperature difference between roof and the soil, the radiation will occur between them. This heat transfer mechanism will be simulated by using the basic radiation equation.
- Convection heat transfer between the roof and the air inside the collector: by solving the energy equation for air inside the collector, this heat transfer will be considered. As it is obvious, the computational mesh should be finer near the wall to capture the thermal and viscosity boundary layer.

4.3.2. Soil

- Sun radiation: As it is stated before, the received energy of the soil from the sun radiation is proportional to the roof transmission coefficient. So, the received energy of the soil can be describe as follow:

$$\text{Absorbed energy from sun radition by soil} = \tau \times q \quad (13)$$

where τ is the transmission coefficient of the roof materials.

- Radiation between the inner surface of the roof with the soil (or absorber): as it is mentioned before, this heat transfer mechanism will be simulated by using the basic radiation equation.
- Convection heat transfer between the soil and the air inside the collector: by solving the energy equation for air inside the collector, this heat transfer will be considered.

4.4. Turbine model

The pressure jump at the turbine is given by the Beetz power limit [15]:

$$\delta p_t = -\frac{8\rho_t U_t^2}{27} \quad (14)$$

Table 2
Comparisons between the numerical results with the experimental data of the Solar Chimney Spanish Prototype [3,4].

Results	Temperature increase in the collector (K)	Air velocity at the base of chimney (m/s)
Experimental	20	15
Numerical	21.8	16.2

The terms ρ_t and U_t are the average air density and the average air velocity at the turbine section, respectively. The output power of the turbine can be calculated by the following equation [16]:

$$\text{Output Power} = \eta_t \delta p_t \forall \quad (15)$$

The terms η_t and $\forall$ are the efficiency of the turbine and the air volume flow rate, respectively. 3-d simulation of turbine can provide more detailed results [17]. However, in this study due to the scope of the Iranian SCPP project, Eq. (15) is used to simulate the turbine output.

4.5. Solution methods

In the Boussinesq approach the density difference is just considered in the gravitational body force. The reference value of density is equal to its value in the ambient temperature. To solve governing equations, Fluent commercial software is used. First order implicit scheme is used to discretize equations in the time frame. To couple velocity and pressure, SIMPLE algorithm is adopted. Velocity values on the volume surfaces are computed by using second order Upwind estimation. To overcome pressure fluctuations, pressure values on the volume surfaces are computed by using PRESTO method [18].

5. IRAN solar energy maps based on NRI method [11]

This atlas which can provide monthly, seasonal and annual values presents the solar energy potential of Iran in GIS software. Iran solar energy maps have various applications in power generation (feasibility study of grid connected/stand alone solar power plants construction), buildings (estimation of thermal/cooling loads and feasibility of applying solar water heater collectors), meteorological and other related fields.

In the mentioned method, the solar energy is calculated based on the altitude angle, cloud factor and declination angle parameters. To determine received and extracted energy values by different solar systems, the solar incidence angle and some parameters about the efficiency of solar systems should be defined. Measured meteorological parameters using in this atlas have been achieved from 217 IRIMO synoptic stations for at least 3 years.

6. Numerical results

6.1. Verification

In order to get confidence about the numerical procedure and undertaken assumptions, we have considered the Solar Chimney Spanish Prototype [3]. The air temperature increase in the collector and the air average velocity at the chimney base are available experimental data of the Spanish prototype. The experimental results indicate that, when the solar radiation is 1000 W/m^2, the upwind velocity at the chimney base is 15 m/s, and the temperature increase through the collector with no-load condition reaches 20 K [3,4]. As it is shown in Table 2, good agreement was obtained between the obtained numerical results and the reported experimental data of the Manzanares prototype [3,4].

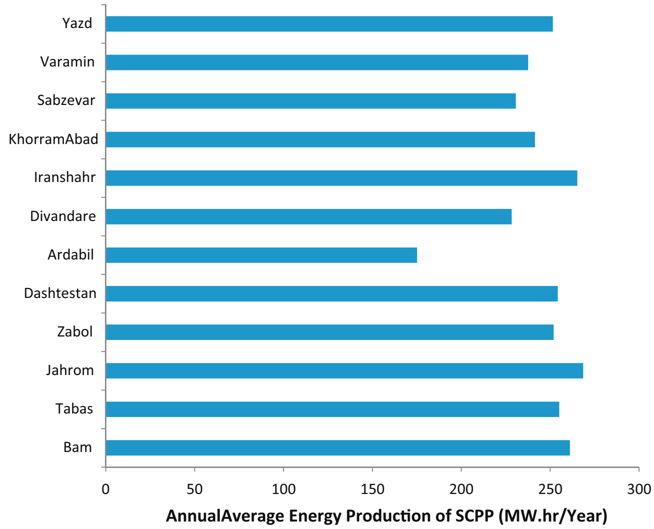


Fig. 5. Annual electrical power generation of SCPP in the selected regions of Iran.

Due to the assumption that the earth surface does not have heat transfer with the earth deeper layers, the ideal absorption assumption [19]; the temperature increase in the numerical results is more than the experimental data. Thereby, the average velocity of numerical results will be more than the experimental data.

6.2. Performance of SCPP in the selected regions

Fig. 5 shows the yearly power output from the reference SCPP at various locations of Iran which conditions are presented in Table 1. As expected, the power output profile is uniform and proportional with solar radiation profile. Among the considered regions, Bam, Jahrom, Dashtestan and Iranshahr have higher power generation per year. Results show that SCPP can produce from 175 to 265 MWh/year in the selected regions.

One of the disadvantages of SCPP is the low energy conversion efficiency [20]. Most of the absorbed solar energy by the SCPP exit from the chimney out let. The air flow at the chimney exit has about 20–30 K difference with the environment. In Fig. 6, the annual energy losses from the chimney outlet for the selected regions have been presented. Comparing the annual energy loss, Fig. 6, to the

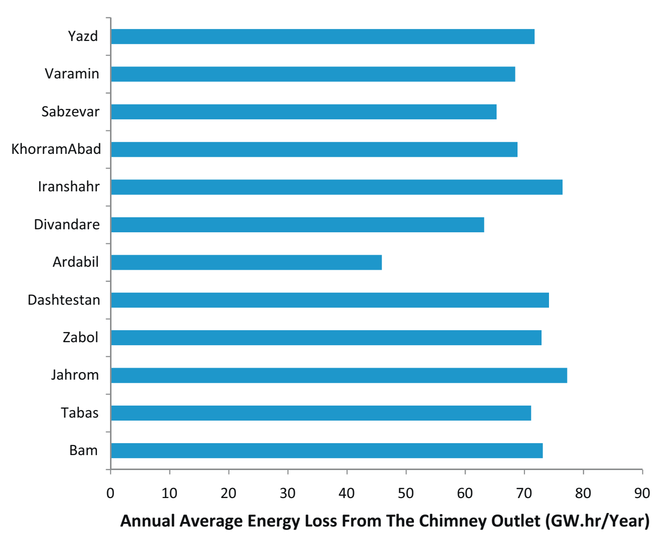


Fig. 6. Annual energy losses from the chimney outlet of SCPP in the selected regions of Iran.

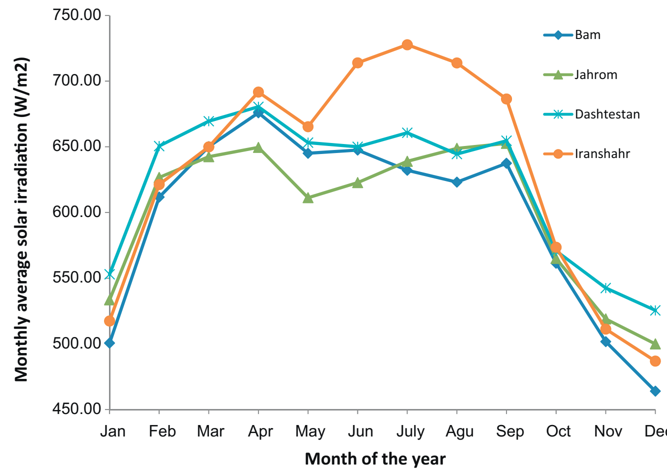


Fig. 7. Monthly average variations of global solar irradiance at four locations in Iran versus month.

annual energy generation of SCPP, Fig. 5, shows that SCPP have total efficiency lower than 4 percent.

To analyze performance of SCPP in details, four regions have been selected for further comparisons which have higher annual electrical power generation based on Fig. 5. The global solar radiations at four locations versus month are shown in Fig. 7. Among these four regions, Iranshahr has higher solar radiation while three other show similar variations during the year. Atmospheric temperature variations of these four regions show similar behaviors, Fig. 8. Maximum ambient temperatures are observed in June, July, and August.

In the simulations, it is assumed that the turbine can create 120 Pa pressure difference. The fixed pressure difference is implemented by using the reverse fan boundary condition. For further research, it is possible to consider that the pressure difference varies between 80 and 400 Pa [16].

The mass flow rates at the chimney exit are presented in Fig. 9. In Fig. 10, electrical power generation of SCPP in four selected regions is shown. In two third of the year, mass flow rates of SCPP have almost similar values while in the June, July, august and September Iranshahr SCPP shows much higher values. Although the mass flow rate of Iranshahr SCPP is higher, its power production is lower. The main reason is that sunshine durations during the mentioned months are higher in other three locations.

In Fig. 10, the trend line of monthly power generation is plotted. The equation is a second order polynomial equation which equation

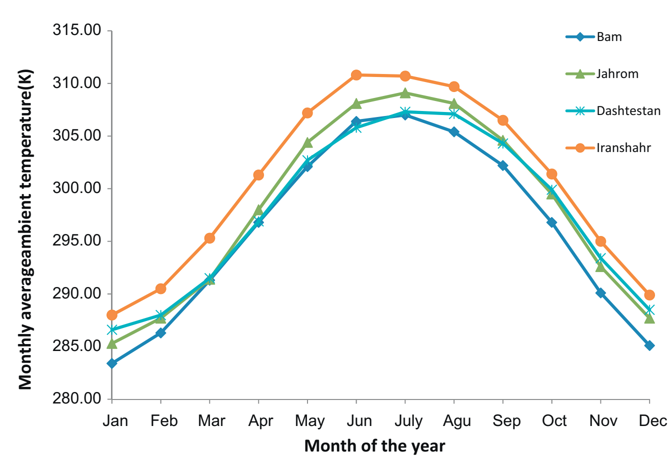


Fig. 8. Monthly average variations of ambient air temperature at four locations in Iran versus month.

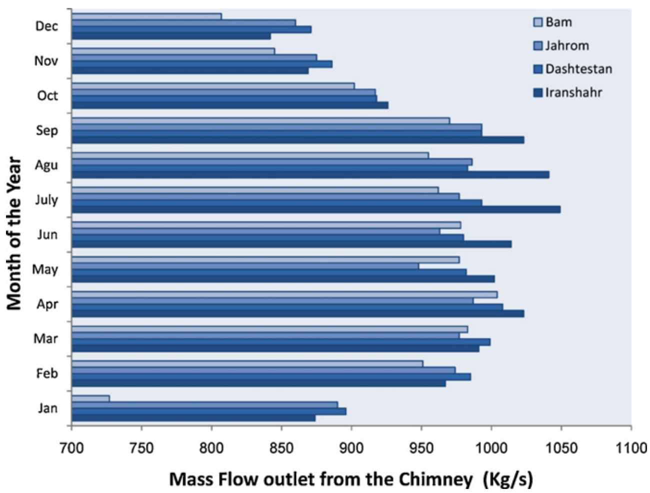


Fig. 9. Mass flow rate at the chimney exit at four locations in Iran versus month.

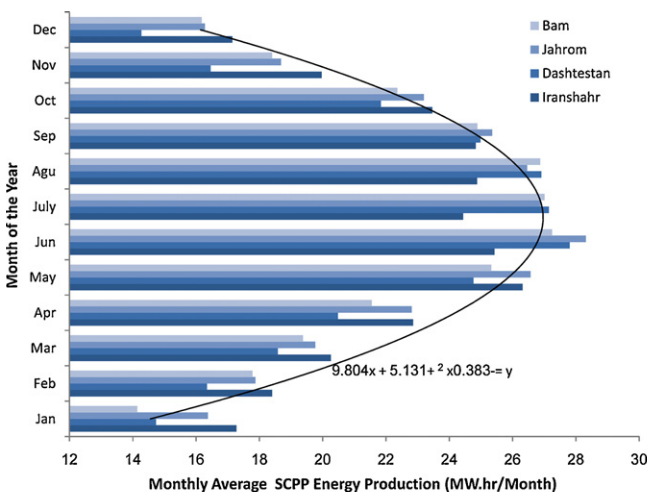


Fig. 10. Monthly average SCPP power generation at four locations in Iran.

can be used as the basis for initial power profile estimations of SCPP in four selected regions.

7. Conclusion

In this work a numerical model has been developed to simulate SCPP performance in difference regions of Iran. The solar chimney is considered to provide the electrical demand of the off-grid villages and to be used as an agricultural greenhouse. The obtained results show that:

- The power generation of a solar chimney in central and southern regions is higher than other regions in Iran due to the higher annual solar irradiation, and higher sunshine durations.
- By increasing the solar irradiations and reduction of heat transfer loss from the chimney roof, mass flow rate will be increase and consequently the power generation will increase.
- Power generation is proportional to chimney mass flow rate and the sunshine durations. As it is shown in Fig. 9 and for example in July, Iranshahr SCPP has higher chimney mass flow rate but due to the lower sunshine duration, it produce lower electrical power comparing with three other locations.
- For further research, the bottom of the collector could be considered as a porous media. Moreover, the water tank energy storage system or salt ponds can be considered in the simulation to provide the power generation throughout the day uniformly.
- For the given climate conditions, the produced electrical power increases with the increase in the solar irradiation and the ambient temperature. The power production is more influenced by the solar irradiation than the ambient temperature.
- One of the SCPP disadvantages is the low overall efficiency, below 4 percent. Results show that almost 96 percent of sun irradiation absorbed energy will lose from the chimney outlet. More study should be taken to increase the SCPP efficiency by using the chimney warmed mass flow outlet.
- Obtained formula for SCPP power generation, Fig. 10, can be used for further general SCPP feasibility study. Projects like MED-CSP can consider this formula which is developed for central and southern regions of Iran.
- There is vast desert land, abundant solar radiation, and high amount of solar irradiation in central and southern regions of Iran. Therefore these regions are suitable for construction sites of SCPP for utilizing local solar irradiation.
- The power output of SCPP in central and southern regions is far more than from that of the same latitude regions in other areas of country. The result may be attributed to the high solar radiation and high sunshine duration during the year
- According to the monthly average environmental data, the considered solar chimney power plant can produce electrical power up to 28 MWh in different months of the year. This electrical power production will be sufficient to meet the power demands of the off-grid villages. Moreover, the collector can be used as a green house for agricultural uses to improve people economical conditions in this area.

References

[1] Zhou X, Wang F, Ochieng RM. A review of solar chimney power technology. Renewable and Sustainable Energy Reviews 2010;14:2315–38.
[2] Nizetic S, Ninic N, Klarin B. Analysis and feasibility of implementing solar chimney power plants in the Mediterranean region. Journal of Energy 2008;33(168):0–1690.
[3] Haaf W, Friedrich K, Mayer G, Schlaich J. Solar chimneys. International Journal of Energy Research 1983;2:3–20.
[4] Haaf W, Friedrich K, Mayer G, Schlaich J. Solar chimneys. International Journal of Energy Research 1984;2:141–61.
[5] Schlaich J, Bergermann R, Schiel W, Weinrebe G. Design of commercial solar updraft tower systems – utilization of solar induced convective flows for power generation. Journal of Solar Energy Engineering 2005;127(February).
[6] Koonsrisuk A, Chitsomboon T. A single dimensionless variable for solar chimney power plant modeling. Solar Energy 2009;83:2136–43.
[7] Pasumarthi N, Sherif SA. Experimental and theoretical performance of a demonstration solar chimney model—Part I. Mathematical model development. International Journal of Energy Research 1998;22:277–88.
[8] Pasumarthi N, Sherif SA. Experimental and theoretical performance of a demonstration solar chimney model—Part II. Experimental and theoretical results and economic analysis. International Journal of Energy Research 1998;22:443–61.
[9] Dai a YJ, Huang HB, Wang RZ. Case study of solar chimney power plants in Northwestern regions of China. Renewable Energy 2003;28:1295–304.
[10] Sangi R. Performance evaluation of solar chimney power plants in Iran. Renewable and Sustainable Energy Reviews 2012;16(January (1)):704–10.
[11] Haghparast-Kashani A, Saleh-Izadkhast P, Lari H-R. Development of optimum solar irradiation energy model for Iran. International Journal of Global Energy Issues 2009;31(2):132–49.
[12] Chergui T, Larbi S, Bouhdjar A. Thermo-hydrodynamic aspect analysis of flows in solar chimney power plants—a case study. Renewable and Sustainable Energy Reviews 2010;14:1410–8.
[13] Pastohr H, Kornadt O, Gurlebeck K. Numerical and analytical calculations of the temperature and flow field in the upwind power plant. International Journal of Energy Research 2004;28(3):495–510.
[14] Larbi S, Bouhdjar A, Chergui T. Performance analysis of a solar chimney power plant in the southwestern region of Algeria. Renewable and Sustainable Energy Reviews 2010;14:470–7.
[15] Sangi R, Amidpour M, Hosseinizadeh B. Modeling and numerical simulation of solar chimney power plants. Solar Energy, vol. 85. Elsevier; 2011. p. 829–38.

[16] Xu G, Ming T, Pan Y, Meng F, Zhou C. Numerical analysis on the performance of solar chimney power plant system. Energy Conversion and Management 2011;52:876–83.
[17] Ming T, Liu W, Xu G, Xiong Y, Guan X, Pan Y. Numerical simulation of the solar chimney power plant systems coupled with turbine. Renewable Energy 2008;33:897–905.
[18] Fluent Inc. Fluent user's guide; 2006.
[19] Ming T, Liu W, Pan Y, Xu G. Numerical analysis of flow and heat transfer characteristics in solar chimney power plants with energy storage layer. Energy Conversion and Management 2008;49:2872–9.
[20] Zhou X, Wang F, Fan J, Ochieng RM. Performance of solar chimney power plant in Qinghai-Tibet Plateau. Renewable and Sustainable Energy Reviews 2010;14:2249–55.